Available online at www.sciencedirect.com
SCIENCE DIRECT
Polymer 46 (2005) 9908–9918
polymer
www.elsevier.com/locate/polymer

Pulsed electron beam irradiation of dilute aqueous poly(vinyl methyl ether) solutions

Thomas Schmidt[a,b], Ireneusz Janik[b], Sławomir Kadłubowski[b], Piotr Ulański[b], Janusz M. Rosiak[b], Rudolf Reichelt[c], Karl-Friedrich Arndt[a,*]

[a]*Institute of Physical Chemistry and Electrochemistry, Dresden University of Technology, Mommsenstr. 13, D-01062 Dresden, Germany*
[b]*Institute of Applied Radiation Chemistry, Technical University of Łódź, Wróblewskiego 15, 93-590 Łódź, Poland*
[c]*Institute for Medical Physics and Biophysics, University of Münster, Robert-Koch-Str. 31, D-48149 Münster, Germany*

Received 11 January 2005; received in revised form 26 May 2005; accepted 27 July 2005
Available online 29 August 2005

Abstract

A dilute aqueous solution of the temperature-sensitive polymer, poly(vinyl methyl ether) (PVME), was irradiated by a pulsed electron beam in a closed-loop system. At temperatures, below the lower critical solution temperature (LCST), intramolecular crosslinked macromolecules, nanogels, were formed. With increasing radiation dose D the molecular weights M_w increase, whereas the dimensions (radius of gyration R_g, hydrodynamic radius R_h) of the formed nanogels decrease. The structure of the PVME nanogels was analyzed by field emission scanning electron microscopy (FESEM) and globular structures with $d=(10–30)$ nm were observed. The phase-transition temperature of the nanogels, as determined by cloud point measurements, decreases from $T_{cr}=36$ °C (non-irradiated polymer) to $T_{cr}=29$ °C ($c_p=12.5$ mM, $D=15$ kGy), because of the formation of additional crosslinks and an increase in molecular weights. The same behavior was observed for a pre-irradiated PVME (γ-irradiation) with higher molecular weight due to intermolecular crosslinks. After pulsed electron beam irradiation the molecular weight again slightly increases whereas the dimension decreases. Above $D=1$ kGy the calculated ρ-parameter ($\rho=R_g/R_h$) is in the range of $\rho=0.5–0.6$ that corresponds to freely draining globular structures.

Keywords: Poly(vinyl methyl ether); Pulsed electron beam irradiation; Nanogels

1. Introduction

Hydrogels are networks of hydrophilic polymers that swell in aqueous media with a multiple water up-take in comparison to their mass or volume [1]. In particular, hydrogels that react with a strong change in their swelling degree or mechanical properties on a slight change in a physical property of the surrounding medium (temperature, pH value, ion strength, solvent concentration, etc.) have a high potential of application [2–4]. Temperature-sensitive gels undergo a discontinuous volume phase transition behavior. They are in a highly swollen state at temperatures below a critical temperature. At temperatures above this temperature they are in a shrunken state. The volume phase transition temperature is near to the lower critical solution temperature (LCST) of the corresponding solution of non-crosslinked polymer. The swelling/deswelling kinetics of sensitive hydrogels depend on the inverse square of their dimension [5]. In order to improve the response time, the hydrogel dimension has to be reduced. Therefore, the synthesis of gels in nanometer or micron range is necessary. In the literature [6–10] different definitions of the terms nanogel and microgel are present. Funke et al. [6] use the term microgel for intramolecular crosslinked macromolecules. On the other hand, such intramolecular crosslinked macromolecules were defined as nanogels by several authors [7–11]. The term microgel is often used for intermolecular crosslinked polymers or products of heterogeneous polymerization techniques, e.g. emulsion or precipitation polymerization [12–16]. Recently, many investigations were performed to synthesize temperature-sensitive microgels based on poly(*N*-isopropyl acrylamide) PNIPAAm [12–14] and poly(*N*-vinyl caprolactam) PVCl

* Corresponding author. Tel./fax: +49 351 463 32013.
E-mail address: karl-friedrich.arndt@chemie.tu-dresden.de (K.-F. Arndt).

0032-3861/$ - see front matter © 2005 Published by Elsevier Ltd.
doi:10.1016/j.polymer.2005.07.077

[15,16], respectively. In this work, we use the term nanogels for intramolecular crosslinked macromolecules.

Our investigations are performed on temperature-sensitive poly(vinyl methyl ether) PVME, a hydrophilic polymer with a LCST in aqueous solutions of about 34 °C [17]. The volume phase transition temperature has been determined by several methods, e.g. DSC [18], IR [19], or NMR spectroscopy [20]. Aqueous PVME solutions can be crosslinked to form a macroscopic network (hydrogel) by high-energy radiation (electron beam or γ-rays) at concentrations above the overlap concentration c^* [21–27]. The mechanism of crosslinking initiated by high-energy radiation of PVME in aqueous solutions was studied by pulse radiolysis and electron spin resonance (ESR) spectroscopy [28,29].

Irradiation at low polymer concentrations ($c < c^*$) does not result in the formation of macroscopic networks. Depending on the irradiation parameters (radiation dose D, dose rate D_h, polymer concentration c_p, irradiation temperature T) molecules with different structures can be obtained (long-chain branched polymers, nanogels, or microgels).

A method to synthesize micro-sized hydrogels by irradiation techniques is the simultaneous polymerization and crosslinking of monomers in aqueous emulsions [30,31]. Furthermore, radiation crosslinked microgels were prepared by γ-ray irradiation of aqueous poly(ethylene oxide) PEO solutions [32]. Irradiation with low dose rates (γ-rays) leads to contracted polymer structures due to the inter- and intramolecular crosslinking reaction. Various studies of γ-ray irradiation of low concentrated aqueous solutions of poly(vinyl alcohol) PVA [33–35] and PVME [36] were performed. Furthermore, the irradiation temperature of aqueous solutions of temperature-sensitive polymers strongly influences the obtained structure. Irradiation of the collapsed structure of PVME in diluted aqueous solutions above LCST leads to temperature-sensitive microgel particles having a porous structure [37]. These particles can serve as a template, e.g. for emulsion polymerization of pyrrol. It results in needle-like conductive polymer structures [38].

Increasing the dose rate (e.g. pulsed electron beam irradiation) increases the number of radicals at the polymer chain and changes the properties of the products. Irradiation of diluted aqueous solutions with pulsed electron beams (generation of a large number of radicals on each separate polymer chain in a short time) leads to the intramolecular combination of the produced radicals. In dilute homogeneous solutions (each macromolecule is separated) of poly(vinyl alcohol) PVA [39], poly(vinyl pyrrolidone) PVP [40], and poly(acrylic acid) PAA [41,42] the formation of nanogels occurs.

The aim of the work was the pulsed electron beam irradiation of dilute aqueous PVME solutions of various concentrations to obtain intramolecular crosslinked macromolecules (nanogels). These nanogels were characterized with respect to their molecular weight, dimension, structure, and temperature-sensitivity.

2. Experimental

2.1. Materials

Poly(vinyl methyl ether) PVME was obtained as a 50 wt% aqueous solution from Aldrich Chemical Co. The molecular weight was determined by static light scattering (SLS) in water as $M_w = 65{,}000$ g/mol. The polymer was used without any further purification. A higher molecular weight sample was obtained by γ-ray irradiation of the 50 wt% aqueous solution with a radiation dose of about 30 kGy using a ^{60}Co source. The pre-irradiated PVME sample was characterized by static light scattering and gel permeation chromatography. Its molecular weight was $M_w = 203{,}000$ g/mol. Its polydispersity, determined by GPC in THF (calibration with PS standards), was $M_w/M_n = 3.0$. The intrinsic viscosity of the contracted pre-irradiated PVME sample was measured in THF at $T = 30$ °C to $[\eta]_{branched} = 18.6$ ml g^{-1}. Based on the Kuhn–Mark–Houwink equation [36] a contraction factor was calculated to $g' = [\eta]_{branched}/[\eta]_{linear} = 0.23$.

PVME was dissolved in water by overnight stirring at room temperature (RT). Solutions were prepared with water purified by distillation and subsequent passing through the Nanopure II system (Barnstead, final specific resistance > 17 MΩ cm). Prior to the irradiation, the solutions were filtered through 0.45 μm filters (Minisart, Sartorius). All polymer concentrations c_p are expressed in mol of repeating units ($M = 58.08$ g/mol) per liter.

2.2. Pulsed electron beam irradiation

Pulse irradiations were performed in a closed-loop flow system (Fig. 1) consisting of a solution reservoir, Tygon tubing, a peristaltic pump, and a quartz irradiation cell. Prior to and during the irradiation, polymer solution in the reservoir was being continuously saturated with argon. The polymer solution flows turbulently through the irradiation

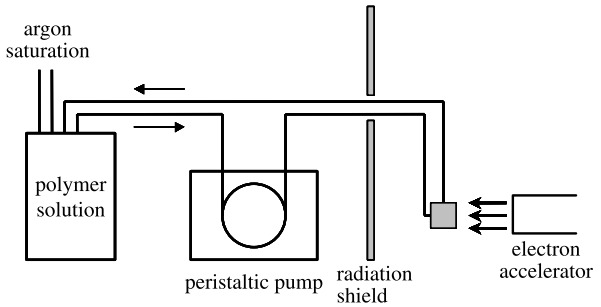

Fig. 1. Schematic illustration of the experimental set-up (closed-loop system).

cell at a rate of 1 ml s^{-1}. During the continuous flow, the cell with an effective volume of 0.7 ml was pulse-irradiated with 6 MeV electrons generated by an ELU-6 linear accelerator (Eksma, Russia). Pulse frequency of 0.5 Hz and pulse duration of 3 μs were applied. The average dose absorbed per single pulse was determined by ferrocyanide dosimetry [43–45] as 0.96 kGy. The average dose for the whole solution volume was calculated based on the number of the applied pulses as well as the known volume of the solution (500 ml) and the irradiation cell (0.7 ml). For details of the preparative pulse radiolysis see Refs. [40,42].

2.3. Static and dynamic light scattering

The weight-average molecular weight M_w, the radius of gyration R_g and the hydrodynamic radius R_h were measured by static and dynamic laser light scattering method with a multi-angle Brookhaven Instruments setup consisting of a Lexel 95E argon ion laser ($\lambda_0 = 514.5$ nm) and a BI-200SM goniometer. Measurements were performed using triple-distilled water as solvent. The samples were filtered through filters of 0.45 μm pore size before the measurement.

The angle and concentration dependence of the scattered light was measured at $T = 25$ °C. Zimm plot algorithm [46] (Eq. (1)) was used to evaluate the scattering data.

$$\frac{K' c_B}{R(q)} = \frac{1}{M_w}\left(1 + \frac{1}{3}R_g q^2\right) + 2A_2 c_P \tag{1}$$

where K' is an optical constant, expressed as $K' = 4\pi^2 n^2 / N_A \lambda_0^2 \, (dn/dc_p)^2$, with N_A, n, dn/dc_p, and λ_0, being Avogadro's number, the refractive index of the solvent, the specific refractive index increment of the solution, and the wavelength of light in vacuum, and $q = (4\pi n/\lambda_0)\sin(\theta/2)$ the scattering vector. The Rayleigh ratio $R(q)$ depends on the polymer concentration c_p and on the scattering angle θ. The extrapolation of $c_p \to 0$ and $\theta \to 0$ provides the weight-average of the molecular weight M_w, the radius of gyration R_g, and the second virial coefficient A_2. The refractive index increment was assumed to be independent of the applied radiation dose and was taken as $dn/dc_p = 0.1438$ ml g^{-1} [37]. The experimental errors of the detected molecular weights and the virial coefficients are in the range of ca. 10–20%. The angle dependence of the scattered light was recorded at $\theta = 30$–$150°$. The determined values of R_g show strong experimental errors, in particular at low concentrations $c_p \leq 25$ mM. Therefore, the values of these concentrations are not discussed in this work.

In dynamic light scattering, the intensity time correlation function $g_2(q,t)$ can be expressed by the Siegert relation (Eq. (2)).

$$g_2(q,t) = A(1 + \beta |g_1(q,t)|^2) \tag{2}$$

where t is the decay time, A the measured baseline, β the coherence factor, and $g_1(q,t)$ the normalized first-order electric field correlation function that is related to the measured relaxation rate Γ (Eq. (3)):

$$g_1(q,t) = \int_0^\infty G(\Gamma) e^{-\Gamma t} d\Gamma \tag{3}$$

The line-width distribution $G(\Gamma)$ can be obtained from the Laplace inversion of $g_1(q,t)$ using CONTIN procedure [47]. For a pure diffusive relaxation, the extrapolation of $q \to 0$ and of $c_p \to 0$ led to the transversal diffusion coefficient D, which is related to the hydrodynamic radius R_h by the Stokes–Einstein equation (Eq. (4)).

$$R_h = \frac{k_B T}{6\pi\eta D} \tag{4}$$

where k_B, T, and η are the Boltzmann constant, the absolute temperature, the viscosity of the solvent, respectively. For dynamic light scattering, no extrapolation of $q \to 0$ and $c_p \to 0$ was performed and an apparent hydrodynamic radius $R_{h,app}$ with an experimental error of ca. 10% was determined at $\theta = 90°$.

2.4. Cloud point measurements

The temperature-sensitivity of the PVME nanogels was analyzed by measuring the UV/VIS absorbance of its aqueous solutions in dependence on the temperature T. UV/VIS spectroscopy was performed with the spectrometer Lambda 35 (Perkin–Elmer) and quartz cuvettes with an optical path of 5.0 mm. Pure water was used as reference for the spectra. The spectra were measured between $\lambda = 200$ nm and $\lambda = 800$ nm with a split of 2 nm. The temperature of the cuvettes was kept constant at each T for 10 min by using a Julabo thermostat (0–80 °C). The transition temperatures were determined as the onset value of the increasing absorption within an experimental error of 10%.

2.5. FESEM measurements

A valuable novel methodical approach for the structural characterization of water-containing materials is the field emission scanning electron microscopy (FESEM) combined with cryo-preparation techniques. The intramolecularly crosslinked nanogel structure was investigated in the swollen state at $T = 25$ °C. A small droplet of the swollen nanogel solution at 25 °C was dropped onto a small fragment of silicon (Si) wafer having a corresponding temperature. The nanogels were physically adsorbed for about 90 s to the Si wafer, before the excess solution was removed with filter paper. Immediately following, the samples were rapidly frozen by plunging into liquid ethane (cooled to $T = -196$ °C) to avoid ice crystal formation (vitreous ice embedding) [48]. Freeze drying was performed within 6 h at $T = -80$ °C and $p = 5 \times 10^{-6}$ Torr using a BAF 300 (Balzers, Principality Liechtenstein) equipped with a turbo molecular pump. After warming up to RT the freeze-dried samples were subsequently rotary shadowed

with 1.5 nm platinum/carbon (Pt/C) at an elevation angle of 65°. The coated samples were examined in a high resolution field emission scanning electron microscope ('in-lens' type, model S-5000, Hitachi Ltd, Tokyo, Japan) in high vacuum ($p = 4 \times 10^{-7}$ Torr) at RT. Micrographs were recorded at 8 kV acceleration voltage using secondary electrons (SE) (for further methodical details of the FESEM, see Refs. [49,50]). For photography the SE micrographs were recorded using Agfapan APX100 film.

3. Results and discussions

When dilute aqueous polymer solutions are subjected to ionizing radiation, hydroxyl radicals are formed, which attack macromolecules by H-atom abstraction and, as a result, carbon-centered polymer radicals are formed. These radicals may decay by disproportion and recombination (crosslinking). Depending on the polymer concentration and on the dose rate two different crosslinking reactions can take place: inter and intramolecular crosslinking (see Fig. 2). If the average numbers of radicals per single chain Z_R is low ($Z_R < 1$), the intermolecular recombination of the formed radicals is observed. Increasing the dose rate (dose D per time t) leads to an increased number of radicals per chain ($Z_R > 1$). In dilute solutions, where the distances between macromolecules are relatively high, the recombination of the formed radicals results mainly in an intramolecularly crosslinking. The crosslinks lead to reduction of the dimension of the macromolecule and nanogels are formed. The resulted nanogels are more resistant to degradation processes, because a degradation of C–C main chain bonds does not reduce their molecular weight [42].

Therefore, in this work dilute aqueous solutions PVME were pulsed electron beam irradiated to obtain intramolecular crosslinked molecules (nanogels). The nanogel formation was studied at two PVME samples of different molecular weights. First, the investigations were performed with the commercially available sample. Furthermore, a two-step crosslinking reaction was used. Irradiation with low dose rates (γ-ray irradiation) at high polymer concentrations increases the molecular weight by intermolecular crosslinking. A following pulsed electron beam irradiation leads to an intramolecular crosslinking.

3.1. Molecular weight of the PVME nanogels

By using static light scattering the weight-average molecular weights M_w of the PVME nanogels in water were determined with respect to the radiation dose D and the polymer concentration c_p. In Fig. 3 the values of M_w of the nanogels obtained by the irradiation at higher concentration ($c_p = 50$–100 mM) are shown.

The molecular weights M_w increase exponentially with increasing radiation dose (Fig. 3(a)), which is typically for polymers that crosslink by high-energy radiation before

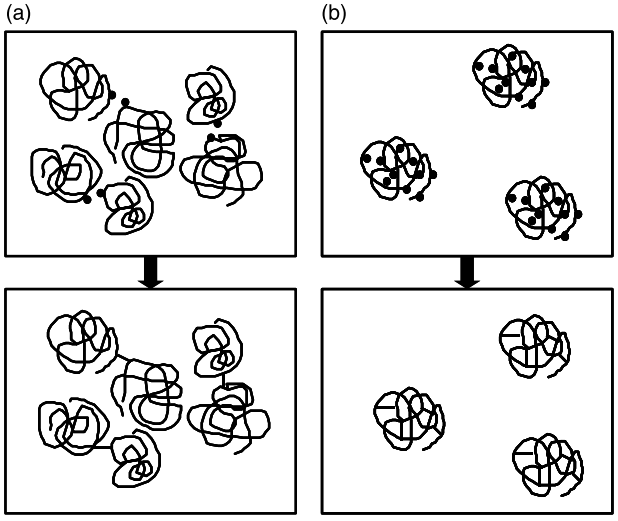

Fig. 2. Influence of the dose rate of the electron beam on the formed polymer structures: (a) medium polymer concentrations and low dose rates lead to intermolecular crosslinking, and (b) low polymer concentrations and high dose pulses lead to intramolecular crosslinking.

reaching the gelation dose D_g. However, this increase in M_w depends on the used concentration. A molecular weight of $M_w \approx (4$–$6) \times 10^6$ g/mol was obtained for the 50 mM solutions at higher doses D in comparison to the 100 mM

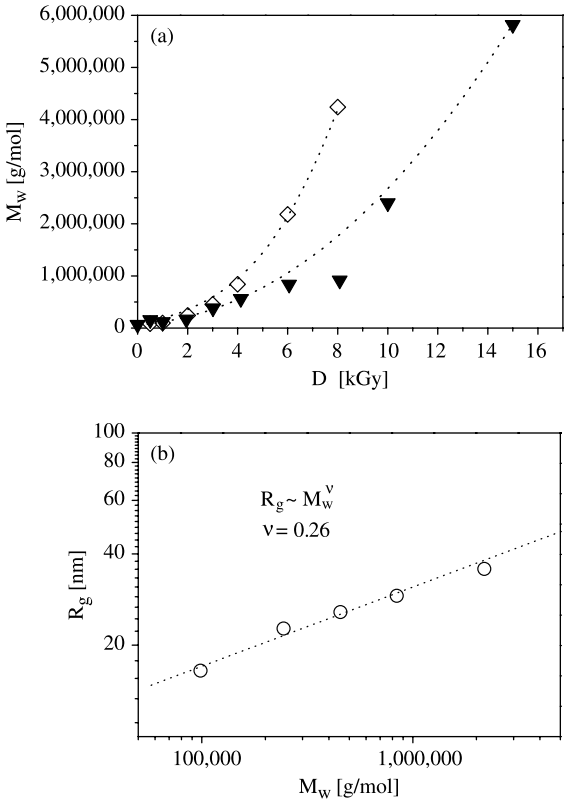

Fig. 3. (a) Molecular weight M_w of the PVME nanogels as a function of the radiation dose D at higher polymer concentrations c_p (▼, 50 mM; ◇, 100 mM). (b) Scaling behavior of M_w and R_g at the highest polymer concentration (100 mM).

solutions. At higher polymer concentrations, but even below the overlap concentration c^*, intermolecular and intramolecular recombination of PVME radicals occurs.

The intermolecular crosslinking is strongly influenced by the distance between neighboring macromolecules, as well as the number of polymeric radicals. The distance can be estimated from the volume of the coiled macromolecule in solution, given by its radius of gyration R_g and the total polymer concentration c_p, respectively. Due to the small distance between PVME molecules in the range of $c_p = 50$–100 mM both, inter and intramolecular recombination of the radicals occurs. In case of the commercially available PVME, the starting molecular weight M_w is almost relatively low, because of the method of synthesis (cationic polymerization). The pulsed electron beam irradiation of such a medium M_w compound usually leads to intermolecular and intramolecular crosslinking occurring side by side and, therefore, to an increase in molecular weight. It can be explained by a relatively low radical concentration at the given polymer chain. Furthermore, the PVME have a rather compact and relatively rigid structure in aqueous solutions, as already discussed by several authors [17,29].

The occurrence of intermolecular crosslinking, leading to a change in the macromolecular structure, is difficult to demonstrate in the discussed case, when both molecular weight and dimension increase upon irradiation. It can be done, however, by analysis of the dimension of the exponent ν of the scaling law $R_g \sim M_w^{\nu}$ of the formed irradiation products (Fig. 3(b)). In case of polymeric coils in good solutions an exponent of $\nu = 0.5$–0.6 should be observed. For hard spheres an exponent of $\nu = 1/3$ should be obtained. The analysis was performed for the highest concentration (100 mM) and an experimental value of $\nu = 0.26$ was obtained. This value is close to that of the spheres within the experimental errors. This finding can be treated as indication that in fact nanogels are formed, having a compact, sphere-like structure.

In the lower concentrations range ($c_p \leq 25$ mM) the dose dependence of M_w (Fig. 4) differs from that observed at higher c_p. Always at low doses ($D \leq 1$ kGy) a strong increase in M_w was observed, that can be explained by the already mentioned rigidity of the relatively low M_w of the starting PVME molecules. This increase in M_w strongly depends on the used polymer concentration. At $D = 1$ kGy the molecular weights are of $M_w = 700{,}000$ g/mol ($c_p =$ 25 mM), $M_w = 400{,}000$ g/mol ($c_p = 17.5$ mM), and $M_w =$ 80,000 g/mol ($c_p = 12.5$ mM), respectively. After applying a radiation dose of $D > 2$ kGy only a slight increase in the molecular weight was observed. In case of low concentrations the intramolecular crosslinking is now the dominating reaction.

3.2. Analysis of the intermolecular crosslinking

In dependence on the radiation dose D structural changes were obtained by different processes. The ratio of crosslinking to degradation reaction strongly depends on D. At low doses D and at low polymer concentrations c_p crosslinking is preferred to main-chain scission. Crosslinking of polymers by irradiation can occur on two different ways: intra and intermolecular. The number of intermolecular crosslinks per volume can be calculated using Eq. (5) [51].

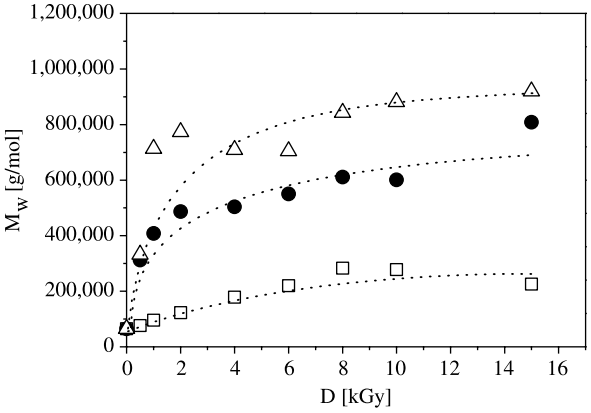

Fig. 4. Molecular weight M_w of the PVME nanogels as a function of the radiation dose D at lower concentrations c_p (□, 12.5 mM; ●, 17.5 mM; △, 25.0 mM).

$$n_C = \frac{1}{2}\left(\frac{1}{M_w^0} - \frac{1}{M_w}\right)c_P \tag{5}$$

where M_w^0 denotes starting molecular weight of the non-irradiated polymer, M_w the molecular weight at various doses D, and c_p the polymer concentration of the irradiated aqueous solution. The calculated n_C values in dependence on the radiation dose D are shown in Fig. 5.

The value of the intermolecular crosslinks n_C increases with increasing polymer concentration c_p at low values of the dose ($D < 2$ kGy). The pulsed electron beam irradiation of PVME solutions at low doses leads always to an intermolecular crosslinking due to the already mentioned

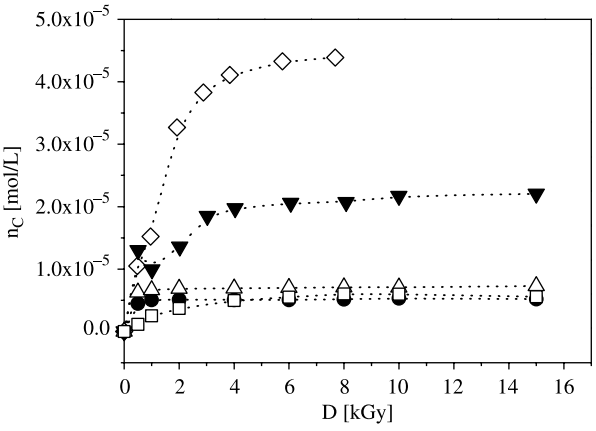

Fig. 5. Number of intermolecular crosslinks per volume n_C of the PVME nanogels as a function of the radiation dose D at different polymer concentrations c_p (□, 12.5 mM; ●, 17.5 mM; △, 25.0 mM; ▼, 50.0 mM; ◇, 100.0 mM).

reasons. Above $D=2$ kGy no significant changes in these values could be observed and irradiation with higher doses leads to the intramolecular crosslinking–polymeric nanogels are formed. The number of intermolecular crosslinks ranges from $n_C=5.5\times10^{-6}$ mol/l (12.5 mM) to $n_C=4.4\times10^{-5}$ mol/l (100 mM). In comparison to our previous studies on γ-irradiated PVME [36] at higher c_p almost the same values of n_C were obtained. At this concentration ($c_p\approx5$ g/l), even below c^*, intermolecular crosslinking is the dominating reaction.

The slope of the functions $n_C=f(D)$ (at low doses D with both, intra and intermolecular crosslinking) corresponds to the values of the radiation-chemical yield of crosslinking G_X and scission G_S.

$$4G_X-G_S=\frac{2c_P}{D\rho}\left(\frac{1}{M_w^0}-\frac{1}{M_w}\right) \quad (6)$$

where D is the absorbed radiation dose (in Gy) and ρ the solution density (in g cm^{-3}). In case of PVME in aqueous solution the polymer undergoes crosslinking reaction, only [29,31]. Therefore, the values of G_S are equal to zero and the equation can be simplified to Eq. (7). The values of G_X were calculated by using Eq. (7) and are shown in Fig. 6.

$$G_X=\frac{c_P}{2D\rho}\left(\frac{1}{M_w^0}-\frac{1}{M_w}\right) \quad (7)$$

Fig. 6 shows an increase in the radiation-chemical yield of crosslinks G_X from $G_X=3.5\times10^{-9}$ mol/J (12.5 mM = 0.725 g/l) to $G_X=1.6\times10^{-8}$ mol/J (100 mM = 5.8 g/l). Janik et al. [29] analyzed the crosslinking behavior of aqueous PVME solutions in a wide range of concentrations c_p. The values of G_X, calculated by using three independent methods, increase with increasing c_p. G_X of the lowest concentration ($G_X\approx3\times10^{-8}$ mol/J at $c_p=20$ g/l), investigated in that study, was only slightly higher than the highest concentration in our study ($G_X=1.6\times10^{-8}$ mol/J at $c_p=$ 5.8 g/l).

3.3. The solution properties of PVME nanogels

Beside the values of M_w and R_g, the SLS measurements give information about the polymer–solvent interactions. The values of second virial coefficient A_2 were analyzed in dependence on the radiation dose D and the polymer concentration c_p (Fig. 7).

Generally, the values of A_2 decrease exponentially with increasing radiation dose D. The interactions within the polymer segments are getting more preferred to the interaction between the polymer segments and the solvent molecules. However, A_2 do not drop below 0. Within the investigated concentrations and dose range, water remains as a good solvent of PVME nanogels. The decrease in A_2 is influenced by both, the increase in molecular weight M_w, as well as the structural changes of the PVME molecules. First, at $D<8$ kGy, A_2 decreases almost independently on c_p with

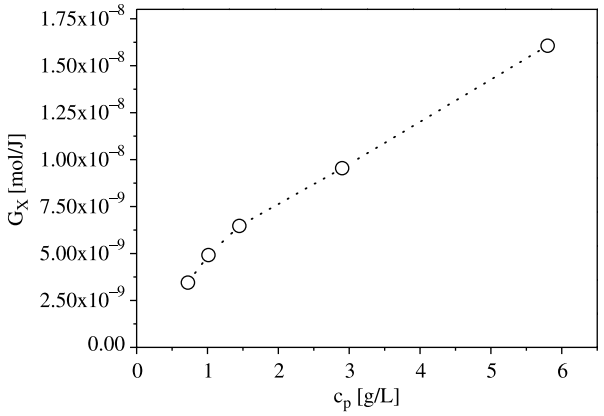

Fig. 6. Radiation-chemical yield of intermolecular crosslinking G_X of the PVME nanogels as a function of the polymer concentration c_p.

increasing radiation dose D resulting from the increasing molecular weight [52]. At doses $D>8$ kGy, the concentration dependence of A_2 becomes more pronounced. On the one hand, M_w increases with increasing D. Therefore, A_2 decrease at a constant D with decreasing c_p. On the other hand, the A_2 value is influenced beside the changes in M_w by structural modifications. The formed internal crosslinks leading to a more compact polymer structure resulting in an additional decrease in the solubility of the PVME nanogels.

3.4. Dimension of the PVME nanogels

Static light scattering techniques allow measuring of the radius of gyration of macromolecules or colloidal particles, if R_g is not smaller than $\lambda/20$ (λ is the wavelength of the incident light). Since R_g of the most nanogels samples synthesized in low-concentration solutions of the commercially available, medium-molecular-weight PVME, was close to or lower than this limit ($\approx$10–20 nm), the calculations of R_g lead to not reliable results. Therefore, the reduction of the dimension of the internally crosslinked macromolecules was followed and discussed by using the

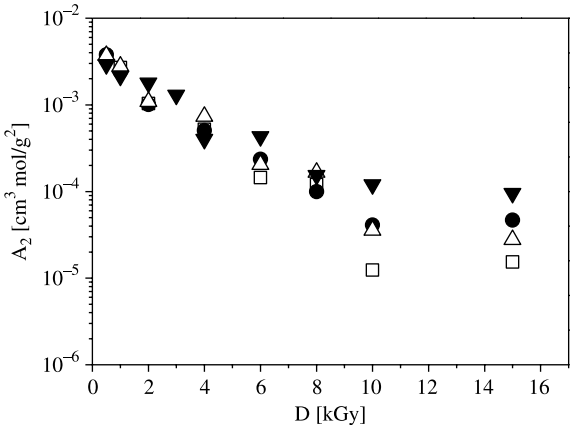

Fig. 7. Second virial coefficient A_2 of the PVME nanogels as a function of the radiation dose D at different polymer concentrations c_p (□, 12.5 mM; ●, 17.5 mM; △, 25.0 mM; ▼, 50.0 mM).

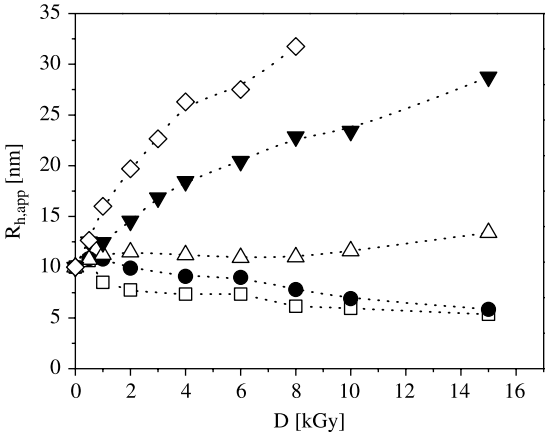

Fig. 8. Apparent hydrodynamic radius $R_{h,app}$ of the PVME nanogels as a function of the radiation dose D at different polymer concentrations c_p (□, 12.5 mM; ●, 17.5 mM; △, 25.0 mM; ▼, 50.0 mM; ◇, 100.0 mM).

data of the hydrodynamic radii $R_{h,app}$ obtained by dynamic light scattering (Fig. 8).

At polymer concentrations $c_p > 25$ mM $R_{h,app}$ increases with increasing radiation dose D (e.g. for $c_p = 50$ mM from $R_{h,app} \approx 10$ nm to $R_{h,app} \approx 30$ nm at $D = 15$ kGy) due to the increase in M_w by the intermolecular crosslinking process. At $c_p = 25$ mM the radius is almost constant at $R_{h,app} \approx 10$ nm despite the increase in molecular weight M_w. At lower concentrations ($c_p < 25$ mM) $R_{h,app}$ decreases with increasing D to a value of $R_{h,app} \approx 5$ nm. The dimension of the PVME nanogels is strongly reduced by the intramolecular crosslinking of PVME, spite of the slight increase in molecular weight M_w. The formed internal chemical bonds prevent strong swelling of the polymer coil in the aqueous solution. This effect is typical for nanogels, also those formed by conventional, chemical intramolecular crosslinking [8,9].

3.5. Temperature-sensitivity of the PVME nanogels

The changes in the molecular weight and the dimension of the PVME nanogels influence the phase-transition temperature T_{cr}. The temperature-sensitivity of the formed nanogels was investigated by using temperature-dependent cloud point measurements. Fig. 9(a) shows the absorbance in the wavelength range of $\lambda = 200$–800 nm of an exemplary nanogel sample in dependence on T.

Usually, the transition temperature of PVME is measured at $\lambda = 500$ nm [53], because of no absorption of PVME at this wavelength. However, in this work the absorbance in the whole range of wavelength was determined (Fig. 9(a)). Plotting the absorbance at various wavelengths versus the temperature allows determining the transition temperature at the onset of the increase in absorption. This absorbance of each nanogel sample increases with increasing temperature. For $\lambda \geq 500$ nm the measured critical temperature T_{cr} is independent on the wavelength. Fig. 9(b) shows the onset

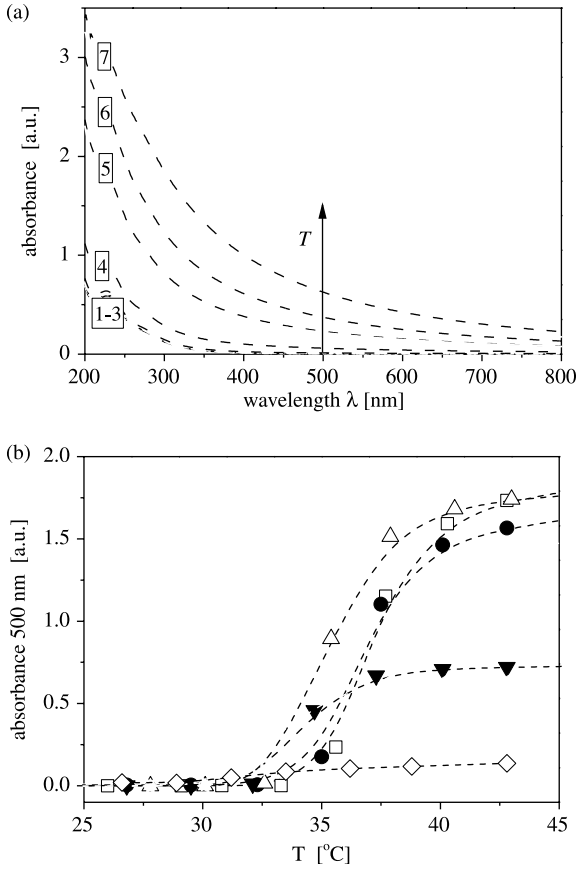

Fig. 9. (a) Example of the temperature-dependent UV/VIS measurements ($c_p = 12.5$ mM, $D = 2$ kGy). Absorption spectra at $\lambda = (200–800)$ nm as a function of the temperature T (1–26.1, 2–31.5, 3–35.0, 4–36.2, 5–38.2, 6–40.3, 7–46.6 °C). (b) Temperature dependence of the absorption at $\lambda = 500$ nm of a PVME nanogel solution ($c_p = 17.5$ mM) as a function of selected radiation doses D (□, 1.0 kGy; ●, 2.0 kGy; △, 4.0 kGy; ▼, 6.0 kGy; ◇, 15.0 kGy).

transition temperature T_{cr} at $\lambda = 500$ nm of the PVME nanogels in dependence on the applied dose D.

The phase-transition temperature T_{cr} of the PVME nanogels decreases with increasing radiation dose D and decreasing polymer concentration c_p (Fig. 10(a)). The phase-transition temperature at a given polymer concentration is influenced by the molecular weight, as well as the structure of the bounded water at the temperature-sensitive polymer chain. To estimate the influence of M_w, T_{cr} was plotted versus M_w (Fig. 10(b)). An almost linear relationship was observed. For higher doses a deviation from the straight line is observed. However, the slope of these functions increases with decreasing polymer concentration c_p indicating an influence of the formed internal crosslinks. The additional internal chemical bonds raise the hydrophobicity of the PVME molecules. The structure of the bonded water molecules at the PVME chain is disturbed. A lower thermal energy is necessary for the breakage of the hydrogen bonds between the hydration shell and the polymer. However, the numbers of additional bonds per each single nanogel is

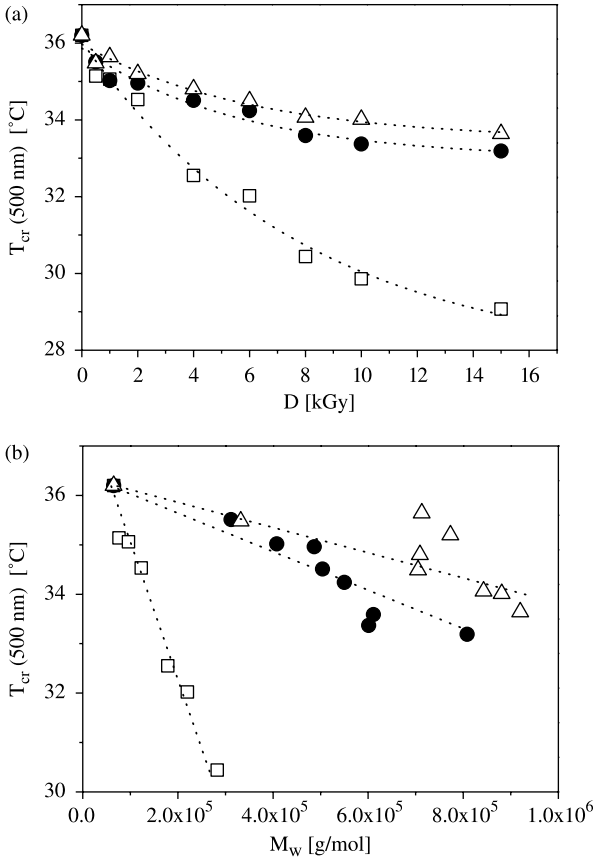

Fig. 10. (a) The critical temperature T_{cr} of the PVME nanogels at $\lambda=$ 500 nm as a function of the polymer concentration c_p (□, 25.0 mM; ●, 17.5 mM; △, 12.5 mM). (b) The critical temperature T_{cr} of the PVME nanogels at $\lambda=500$ nm as a function of the molecular weights M_w (□, 25.0 mM; ●, 17.5 mM; △, 12.5 mM).

relatively small and, therefore, the decrease in the transition temperature T_{cr} is small.

All the experimental results (SLS, DLS, UV/VIS) of the lowest used polymer concentration ($c_p=12.5$ mM) are summarized in Table 1.

3.6. Morphology of the PVME nanogels

For nanogels a globular structure can be assumed, because of a compact structure of the internal crosslinked macromolecule. In [42] the expected sphere-like structure of PAAc nanogels was detected by AFM measurements. In this work electron microscopy (FESEM) combined with cryo-preparation technique was used to visualize the structure of the PVME nanogels. The measurements were performed at an exemplary nanogel in its swollen state at $T=25$ °C.

The technique of cryo-preparation of water containing samples allows visualizing their solid structure after the freeze-drying by electron microscopy without any structural changes during drying process. The FESEM micrographs (Fig. 11) show the structure of the PVME nanogels in the swollen state. Fig. 11(a) and (b) shows a porous 'net' of the

Table 1
Static and dynamic light scattering data and critical temperatures of the PVME nanogels of the lowest polymer concentration ($c_p=12.5$ mM)

$c_p=12.5$ mM	SLS		DLS	UV/VIS
D (kGy)	M_w (g/mol)	A_2 (cm^3 mol/g^2)	$R_{h,app}$ (nm)	T_{cr} (°C)
0.5	76,300	3.53×10^{-3}	10.65	35.14
1.0	96,100	2.70×10^{-3}	8.50	35.06
2.0	123,000	1.04×10^{-3}	7.75	34.53
4.0	179,000	5.24×10^{-4}	7.35	32.55
6.0	220,000	1.45×10^{-4}	7.35	32.02
8.0	283,000	1.20×10^{-4}	6.15	30.44
10.0	278,000	1.24×10^{-5}	5.95	29.86
15.0	226,000	1.54×10^{-5}	5.35	29.07

polymer sample with thin ropes (appr. 50 nm) and clusters of particles. At higher magnifications of the particle cluster (b) and (c) a globular structure of the particles was observed. The diameters of the particles are typically in the range of $d\approx20$–30 nm. In Fig. 11(c) some particles with a larger dimension ($d\approx50$ nm) are shown. In another part of the investigated sample (d) only the small particles are visible.

3.7. Pre-irradiated PVME

Polymers of vinyl ether monomers can only be obtained by cationic polymerization [54]. These polymers (like PVME) have relatively low molecular weights ($M_w<10^5$ g/mol) due to side reactions. Cation transfer reactions to already formed macromolecules lead to a long-chain branching of the polymers. Therefore, the polydispersity of these polymers is relatively high ($M_w/M_n>2$).

A possibility to increase the molecular weight of PVME is the irradiation of its concentrated aqueous solutions. In such conditions the macromolecules crosslink mainly intermolecularly and branched polymers with higher molecular weight are formed. Below the gelation dose D_g no macroscopic network formation occurs and the higher molecular weight polymer remains soluble. Such a pre-irradiated PVME sample with higher molecular weight ($M_w=200{,}000$ g/mol) was also used for the synthesis of nanogels by intramolecular crosslinking initiated by pulsed electron beam irradiation.

The pulsed electron beam experiments on the pre-irradiated PVME were performed only at one concentration ($c_p=10$ mM). This concentration, that is lower than that of the experiments with the commercial PVME, was chosen because the intermolecular distances of the higher M_w polymer in solution are smaller at the same concentrations. Irradiation of this sample in the range $D=0-8$ kGy leads to an increase in molecular weights M_w (Fig. 12). In the range of very low doses ($D=1$ kGy) the molecular weight M_w increases, again (Fig. 4). Between $D=1$ kGy and $D=6$ kGy the molecular weights range from $M_w=1{,}000{,}000$ g/mol to

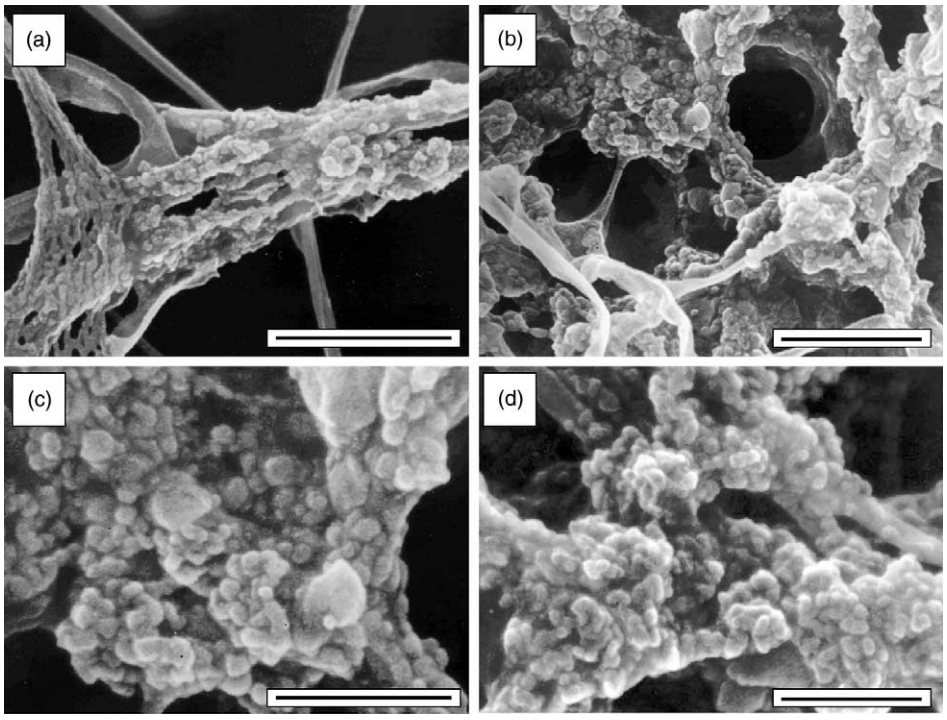

Fig. 11. FESEM micrograph of PVME nanogels (c_p=25.0 mM, D=15 kGy) swollen in water at T=25 °C at different magnifications. The bars correspond to 360 nm ($a+b$), and to 180 nm ($c+d$).

M_w=2,000,000 g/mol, respectively. The increase in molecular weight to M_w=3,500,000 g/mol at a dose of D= 8 kGy is difficult to explain. Probably, the rigidity and the steric hindrance are increased due to the long-chain branching of the intermolecular crosslinked pre-polymer.

The radius of gyration R_g and hydrodynamic radius $R_{h,app}$ of the intermolecular crosslinked sample after pulsed-irradiation are shown in Fig. 13. Both, the R_g and the $R_{h,app}$, increase by the irradiation with D=1 kGy to R_g= 60 nm and $R_{h,app}$=35 nm, respectively. With increasing dose ($D>1$ kGy) the dimensions of these PVME nanogels decrease due to the dominance of the intramolecular linking.

The molecular weights and the radii are high enough for a correct analysis of R_g by light scattering. Independently on the error of the absolute value of R_h (measurements at a scattering angle of 90°), the ρ-parameter ($\rho=R_g/R_h$) was calculated in dependence on the dose (Fig. 14). The calculated ρ-parameter of the non-irradiated sample is ρ= 1.15. It is somewhat lower than that of a polydisperse coil in a good solvent ($\rho=3^{1/2}\approx1.73$) or a polydisperse, long-chain branched macromolecule ($\rho\approx1.225$) [55]. The intermolecular crosslinking of the concentrated PVME solution leads already to a contraction of the molecules (as already recognizable by the determination of the contraction factor g'=0.23). The irradiation of the dilute

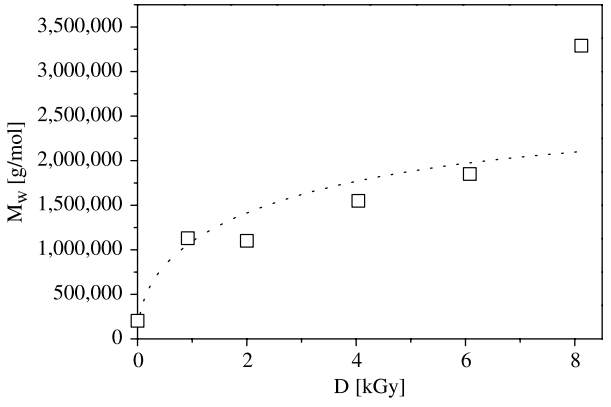

Fig. 12. Molecular weight M_w of PVME nanogels obtained from the pre-irradiated sample as a function of the radiation dose D.

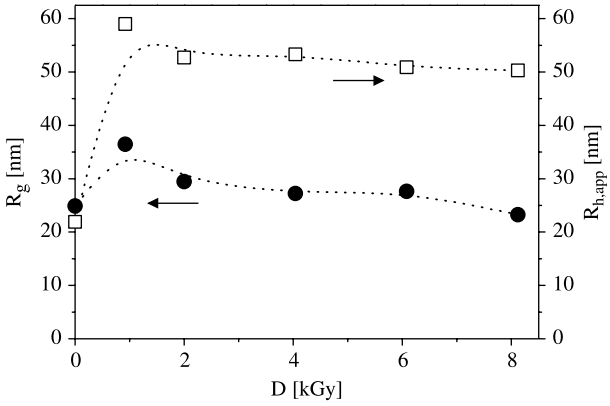

Fig. 13. Dimension (□, radius of gyration R_g, ●, apparent hydrodynamic radius $R_{h,app}$) of the PVME nanogels obtained from the pre-irradiated sample as a function of the radiation dose D.

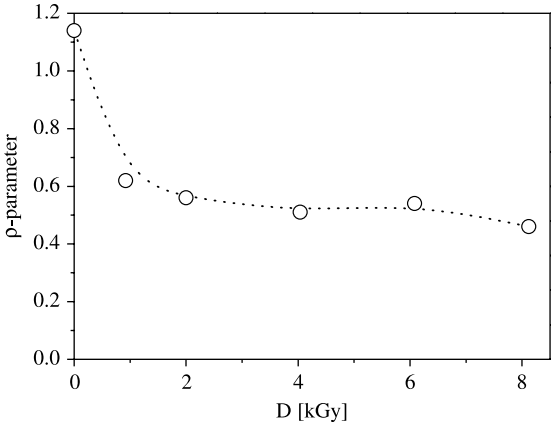

Fig. 14. ρ-parameter of PVME nanogels obtained from the pre-irradiated sample as a function of the radiation dose D.

solutions of these molecules at low D decreases dramatically the ρ-parameter. Above $D=1$ kGy the ρ-parameter decreases moderately to $\rho=0.5$–0.6. In the literature [56] these values were measured for soft globular polymer structures (microgels). On the other hand, the compact structures (hard spheres) would yield higher values ($\rho=(3/5)^{1/2}\approx 0.775$) [55]. The determined values of ρ-parameter are in the range of soft spheres. Therefore, it can be concluded that the formed nanogels have a globular, freely draining structure.

All the results of the nanogels obtained from the pre-irradiated PVME sample are summarized in Table 2.

4. Conclusions

Pulsed electron beam irradiation of aqueous oxygen-free PVME solutions at low temperatures leads at low polymer concentrations ($c_p<25$ mM) to an intramolecular crosslinking reaction of PVME. Temperature-sensitive crosslinked macromolecules (nanogels) with small dimensions ($\approx 10^1$ nm range) could be synthesized. The intramolecular coupling of the polymer radicals strongly depends on the polymer concentration in aqueous solution, the used radiation dose, as well as the starting molecular weight.

In the case of the commercial PVME sample at low radiation doses ($D<2$ kGy) the molecular weight of PVME increases (independently of concentration), because of intermolecular crosslinking of the relatively rigid PVME molecules. At higher concentrations of PVME ($c_p>25$ mM) an increase in both, M_w and dimension in the whole dose range was observed. This is due to the distance between neighboring molecules and a low number of radicals generated at each chain. At lower polymer concentrations ($c_p<25$ mM) no further increase in molecular weight was observed-intramolecular crosslinking reaction occurs. The dimension (hydrodynamic radii) of the internally crosslinked nanogels decreases. By using FESEM measurements a compact, globular particles with diameters of $d=10$–30 nm were determined. The temperature-sensitive behavior of the PVME nanogels was measured by cloud point measurements. The critical temperature T_{cr} decreases with increasing radiation dose due to the increase in molecular weight and a more compact structure of macromolecules. The internal linking bonds disturb the structure of the water shell hydrated the coils that lead to their lower transition temperature T_{cr}.

For a pre-irradiated PVME sample of a higher initial M_w, the irradiation experiments were performed at one concentration ($c_p=10$ mM). Again, an increase in M_w and in radius at a low dose ($D=1.0$ kGy) was observed. However, after a small increase in the dimension (R_g and $R_{h,app}$), the radii are decreasing with increasing radiation does D due the internal crosslinking of the formed macromolecules. The measured radii allow calculating the ρ-parameter. A typical value for microgels of $\rho=0.5$–0.6 independently on the dose was calculated.

Acknowledgements

The authors are grateful to Dr K. Hodyr and Mr B. Jedrzejczak (LINAC, Technical University of łódź) for their technical assistance during the irradiation experiments, and to Mrs U. Keller (University of Münster) for the majority of FESEM studies. T.S. thanks the European Commission within the Marie Curie Host Fellowship for the scholarship (contract number: HPMT-CT-2001-00228). The work was financed by the Deutsche Forschungsgemeinschaft (SFB 287), the Marie Curie Host Fellowship and the International Atomic Energy Agency (POL/6/007).

Table 2
Static and dynamic light scattering data of the PVME nanogels obtained from the pre-irradiated sample ($c_p=10.0$ mM)

Sample	SLS			DLS	$\rho=(R_g/R_{h,app})$
D (kGy)	M_w (g/mol)	R_g (nm)	A_2 (cm^3 mol/g^2)	$R_{h,app}$ (nm)	
0.0	203,000	24.9	1.14×10^{-4}	21.9	1.14
0.92	1,130,000	36.5	1.91×10^{-4}	59.0	0.62
2.00	1,100,000	29.5	7.05×10^{-5}	52.7	0.56
4.04	1,550,000	27.3	5.02×10^{-5}	53.3	0.51
6.08	1,850,000	27.7	8.06×10^{-5}	50.9	0.54
8.12	3,290,000	23.3	4.92×10^{-5}	50.3	0.46

References

[1] Wichterle O, Lim D. Nature 1960;185:117–8.
[2] Peppas NA. Hydrogels in medicine and pharmacy. Boca Raton: CRC Press; 1986.
[3] Lutolf MP, Raeber GP, Zisch AH, Tirelli N, Hubbell JA. Adv Mater 2003;15:888–92.
[4] Richter A, Kuckling D, Howitz S, Gehring T, Arndt KF. J Microelectromech Syst 2003;12:748–53.
[5] Tanaka T, Fillmore DJ. J Chem Phys 1979;70:1214–8.
[6] Funke W, Okay O, Joos-Müller B. Adv Polym Sci 1998;136:139–234.
[7] Graham NB, Cameron A. Pure Appl Chem 1998;70:1271–5.
[8] Frank M, Burchard W. Makromol Chem, Rapid Commun 1991;12: 645–52.
[9] Brasch U, Burchard W. Macromol Chem Phys 1996;197:223–35.
[10] Baker WO. Ind Eng Chem 1949;41:511–20.
[11] Ulanski P, Rosiak JM. Polymeric nano/microgels. In: Nalwa HS, editor. Encyclopedia of nanoscience and nanotechnology, vol. VIII. Stevenson Ranch, CA: American Scientific Publishers, 2004. p. 845–71.
[12] Pelton R. Adv Colloid Interf Sci 2000;85:1–33.
[13] Senff H, Richtering W. J Chem Phys 1999;111:1705–11.
[14] Wu C, Zhou S. Macromolecules 1996;29:1574–8.
[15] Gao Y, Au-Yeung SCF, Wu C. Macromolecules 1999;32:3674–7.
[16] Boyko V, Pich A, Lu Y, Richter S, Arndt KF, Adler HJP. Polymer 2003;44:7821–7.
[17] Horne RA, Almeida JP, Day AF, Yu NT. J Colloid Interf Sci 1971;35: 77–84.
[18] Schäfer-Soenen M, Moerkerke R, Koningsveld R, Berghmans H, Dušek K, Šolc K. Macromolecules 1997;30:410–6.
[19] Maeda Y. Langmuir 2001;17:1737–42.
[20] Hanyková L, Spěváček J, Ilavský M. Polymer 2001;42:8607–12.
[21] Kabra BG, Akhtar MK, Gehrke SH. Polymer 1992;33:990–5.
[22] Suzuki M, Hirasa O. Adv Polym Sci 1993;110:241–61.
[23] Kishi R, Ichijo H, Hirasa O. J Int Mater Syst Struct 1993;4:533–7.
[24] Moerkerke R, Meussen F, Koningsveld R, Berghmans H, Mondelaers W, Schacht E, et al. Macromolecules 1998;31:2223–9.
[25] Arndt KF, Schmidt T, Menge H. Macromol Symp 2001;164:313–22.
[26] Schmidt T, Querner C, Arndt KF. Nucl Instrum Methods Phys Res B 2003;208:331–5.
[27] Janik I, Kasprzak E, Al-Zier A, Rosiak JM. Nucl Instrum Methods Phys Res B 2003;208:374–9.
[28] Janik I, Ulański P, Rosiak JM, von Sonntag C. J Chem Soc, Perkin Trans 2 2000;2034–40.
[29] Janik I, Ulański P, Hildenbrand K, Rosiak JM, von Sonntag C. J Chem Soc, Perkin Trans 2 2000;2041–8.
[30] Sáfrány A, Kano S, Yoshida M, Omichi H, Katakai R, Suzuki M. Radiat Phys Chem 1995;46:203–6.
[31] Graselli M, Smolko E, Harigittai P, Sáfrány A. Nucl Instrum Methods Phys Res B 2001;185:254–61.
[32] Schnabel W, Borgwardt U. Makromol Chem 1969;123:73–9.
[33] Wang B, Mukataka S, Kodama M, Kokufuta E. Langmuir 1997;13: 6108–14.
[34] Wang B, Kodama M, Mukataka S, Kokufuta E. Polym Gels Networks 1998;6:71–81.
[35] Wang B, Mukataka S, Kokufuta E, Kodama M. Radiat Phys Chem 2000;59:91–5.
[36] Querner C, Schmidt T, Arndt KF. Langmuir 2004;20:2883–9.
[37] Arndt KF, Schmidt T, Reichelt R. Polymer 2001;42:6785–91.
[38] Pich A, Lu Y, Adler HJP, Schmidt T, Arndt KF. Polymer 2002;43: 5723–9.
[39] Ulański P, Janik I, Rosiak JM. Radiat Phys Chem 1998;52:289–94.
[40] Ulański P, Rosiak JM. Nucl Instrum Methods Phys Res B 1999;151: 356–60.
[41] Ulański P, Kadłubowski S, Rosiak JM. Radiat Phys Chem 2002;63: 533–7.
[42] Kadłubowski S, Grobelny J, Olejniczak W, Cichomski M, Ulański P. Macromolecules 2003;36:2484–92.
[43] Rabani J, Matheson MS. J Phys Chem 1966;70:761–9.
[44] Broszkiewicz R. Chemical methods of dosimetry of ionising radiation. Warsaw: WNT; 1971.
[45] Schuler RH, Hartzell AL, Behar B. J Chem Phys 1981;85:192–9.
[46] Zimm BH. J Chem Phys 1948;16:1099–116.
[47] Provencher SW. Makromol Chem 1979;180:201–9.
[48] Dubochet J, Chang JJ, Freeman R, Lepault J. Ultramicroscopy 1982; 10:55–61.
[49] Pawley JB. Adv Electr Electron Phys 1992;83:203–74.
[50] Reimer L. Image formation in low voltage scanning electron microscopy. Bellingham: SPIE Optical Engineering Press; 1993.
[51] Charlesby A. Atomic radiation and polymers. Oxford: Pergamon Press; 1960.
[52] Nordmeier E, Lechner MD. Polym J 1989;21:623–32.
[53] Ichijo H, Hirasa O, Kishi R, Oowada M, Sahara K, Kokufata E, et al. Radiat Phys Chem 1995;46:185–90.
[54] Nuyken O, Crivello J. Poly(vinyl ether)s, poly(vinyl ester)s, and poly(vinyl halogenide)s. In: Kricheldorf HR, editor. Handbook of polymer synthesis. New York: Dekker; 1989.
[55] Burchard W, Schmidt M, Stockmayer WH. Macromolecules 1980;13: 1265–72.
[56] Schmidt M, Nerger D, Burchard W. Polymer 1979;20:582–8.